International Journal on Recent and Innovation Trends in Computing and Communication
ISSN: 2321-8169 Volume: 10 Issue: 7
Article Received: *25 April 2022* ***Revised:*** *12 May 2022* ***Accepted:*** *30 June 2022*

Laser Beam Welding for Heat-Resistant Ni Superalloys: A 50-Year Review

Suman Kumar Saurabh[1] , Ashutosh Kumar [2*]

[1,2*]Department of Mechanical Engineering, National Institute of Technology, Jamshedpur-831014

*Corresponding author- ashu101634@gmail.com

Abstract

Laser beam welding (LBW) has become indispensable for joining high-temperature Ni-based superalloys like Inconel and Hastelloy, critical for aerospace, nuclear, and advanced power systems. This review charts the progress of laser welding these alloys from 1970 to 2022, focusing on process physics, metallurgical shifts, defect origins, and strategies for reliable joints. Compared to conventional arc welding, LBW shines by delivering low heat input, slim heat-affected zones (HAZ), and superior dimensional control—key for precision parts. We dissect core phenomena: rapid solidification microstructures, Nb segregation, Laves phase formation, liquation cracking, and γ′/γ″ precipitation dynamics, which dictate weld integrity. Optimisation takes centre stage, exploring parameter tuning, beam oscillation for homogeneity, residual stress mitigation, post-weld heat treatments (PWHT), fatigue enhancements, and digital tools. Emerging frontiers include AI-guided control and digital twins for real-time prediction and simulation. Synthesising five decades of science and industry, this work reveals how LBW evolved from experimental curiosity to production powerhouse. Challenges like hot cracking persist, but innovations promise breakthroughs. Looking ahead, hybrid beams, in-situ monitoring, and machine learning will drive welds resilient to extreme environments—pushing boundaries in turbine blades, reactor components, and beyond.

Keywords: Laser beam welding; Ni-based superalloys; Inconel 718; Hastelloy X; High-energy-density welding

1. Introduction

Welding is a critical manufacturing process that permanently joins materials by applying heat, pressure, or a combination of both. Since the early twentieth century, welding technologies have evolved from conventional gas and arc-based methods to highly sophisticated high-energy-density processes capable of joining advanced engineering materials with precision and reliability [1]. The increasing demand for lightweight, high-strength, and high-temperature components in aerospace, nuclear, petrochemical, and power generation industries has accelerated the development of advanced welding techniques capable of processing difficult-to-weld alloys [2]. Among structural materials designed for extreme environments, nickel-based superalloys represent one of the most important classes of high-temperature-resisting alloys. These materials, including commercial grades such as Inconel 718, Inconel 625, and Hastelloy X, exhibit exceptional mechanical strength, creep resistance, fatigue performance, and oxidation resistance at elevated temperatures exceeding 700–1000 °C [3]. Their superior performance arises from complex microstructural features such as γ (austenitic matrix), γ′ ($Ni_3(Al,Ti)$), and γ″ (Ni_3Nb) precipitates, solid-solution strengthening, and carbide formation [4]. However, these same strengthening mechanisms that provide excellent high-temperature properties also introduce challenges during welding, including hot cracking, microsegregation, liquation cracking in the heat-affected zone (HAZ), and residual stress development [5].

Traditional arc welding processes such as gas tungsten arc welding (GTAW) and gas metal arc welding (GMAW) have been widely used for joining nickel-based superalloys. While these methods are cost-effective and versatile, they are associated with relatively large heat input, wide heat-affected zones, distortion, and susceptibility to weld defects [6]. The thermal cycles produced by arc welding can significantly alter the precipitation state and grain structure of superalloys, thereby compromising high-temperature mechanical properties [7]. As component complexity increases and performance requirements become more stringent, alternative joining technologies with greater precision and lower heat input have become necessary.

High-energy-density welding (HEDW) processes emerged as a solution to these limitations. Characterized by extremely concentrated heat sources and high power densities, HEDW techniques enable deep penetration welding with narrow fusion zones and minimal thermal distortion [8]. The two most prominent high-energy welding technologies are electron beam welding (EBW) and laser beam welding (LBW). EBW was initially developed and widely applied in aerospace applications in the 1960s and 1970s for joining high-performance alloys under vacuum conditions [9]. Although EBW provides excellent penetration depth and weld quality, its requirement for vacuum chambers limits its flexibility for large-scale industrial applications.

Laser beam welding, on the other hand, has evolved into a highly versatile and efficient joining process capable of operating in atmospheric conditions with high precision [10]. The fundamental principle of LBW involves focusing a coherent laser beam onto the workpiece surface, producing localized melting and fusion. Depending on the power density and interaction time, the welding process may operate in conduction mode or keyhole mode. In conduction mode, energy absorption leads to shallow weld penetration, whereas keyhole mode involves vaporization-induced cavity formation that enables deep penetration and high aspect ratio welds [11]. The development of high-power CO_2 lasers in the 1970s, Nd:YAG lasers in the 1980s, and fiber and disk lasers in the 2000s has progressively enhanced beam quality, energy efficiency, and process control [12].

For nickel-based superalloys, LBW offers several advantages over conventional welding processes. The concentrated heat source results in rapid solidification rates, refined microstructures, and reduced heat-affected zones [13]. Lower total heat input minimizes distortion and residual stress accumulation, which are critical considerations for aerospace turbine blades, combustor liners, and heat exchanger components [14]. Furthermore, the flexibility of beam delivery systems enables automation and integration with modern manufacturing systems, including robotic welding and Industry 4.0 frameworks [15].

Despite these advantages, welding of nickel-based superalloys using laser technology is not without challenges. Rapid cooling rates can exacerbate solidification cracking, particularly in alloys with high Nb or Mo content such as Inconel 718 and Hastelloy X [16]. Microsegregation of alloying elements during solidification can lead to the formation of brittle Laves phases, which reduce ductility and creep performance [17]. Additionally, porosity formation due to keyhole instability or gas entrapment remains a critical concern in high-power laser welding processes [18]. Therefore, careful control of process parameters—including laser power, welding speed, focal position, shielding gas composition, and beam oscillation—is essential to achieve defect-free and mechanically reliable joints.

Over the past five decades, research on laser welding of nickel-based superalloys has progressed from exploratory laboratory investigations to sophisticated multi-physics modeling and industrial implementation. Early studies in the 1970s and 1980s focused primarily on feasibility and basic metallurgical characterization [9,12]. The 1990s saw the integration of numerical simulation techniques to predict thermal fields and residual stresses [19]. The introduction of fiber lasers in the early 2000s marked a significant advancement due to improved beam quality and electrical efficiency [20]. More recently, hybrid laser-arc welding techniques, in-situ monitoring systems, and artificial intelligence-based parameter optimization have further enhanced process reliability and productivity [21,22].

In parallel with process development, substantial efforts have been directed toward understanding microstructural evolution in laser-welded superalloys. The rapid solidification inherent to LBW produces dendritic microstructures with segregation patterns distinct from those formed during arc welding [23]. Post-weld heat treatment (PWHT) is often employed to homogenize microstructures and restore precipitation hardening phases [24]. Mechanical performance assessments—including tensile strength, fatigue life, creep resistance, and fracture toughness—have demonstrated that optimized laser welds can achieve properties comparable to or even exceeding those of base materials [25].

Another important development is the integration of LBW with additive manufacturing (AM) processes. Additively manufactured nickel-based components frequently require joining or repair operations. Laser welding offers compatibility with AM microstructures and enables repair of high-value aerospace components with minimal distortion [26]. Research in the 2015–2022 period has increasingly focused on the interaction between additive microstructures and laser welding thermal cycles, revealing opportunities for microstructural tailoring and grain refinement [27].

International Journal on Recent and Innovation Trends in Computing and Communication
ISSN: 2321-8169 Volume: 10 Issue: 7
Article Received: *25 April 2022* ***Revised:*** *12 May 2022* ***Accepted:*** *30 June 2022*

The industrial relevance of laser welding for nickel-based superalloys continues to expand. Gas turbine engines, rocket propulsion systems, nuclear reactors, and chemical processing equipment rely heavily on these alloys for performance in aggressive environments [28]. As global energy demands increase and environmental regulations become stricter, the need for efficient, high-temperature systems intensifies, further emphasizing the importance of reliable joining technologies.

From a manufacturing perspective, process optimization plays a pivotal role in ensuring weld strength and joint reliability. Modern approaches combine experimental design, statistical modeling, computational fluid dynamics (CFD), and real-time monitoring to establish robust process windows [29]. Emerging technologies such as beam shaping, dual-beam welding, and oscillating laser techniques aim to control melt pool dynamics and reduce defect formation [30]. The integration of machine learning algorithms for parameter prediction represents a promising frontier in welding science [22].

Given the rapid technological advancements and expanding application scope, a comprehensive review of laser beam welding of nickel-based superalloys is timely and necessary. While numerous studies have examined specific alloys or process conditions, there remains a need for an integrated assessment covering historical development, process fundamentals, metallurgical phenomena, optimization strategies, and future research directions. This review therefore aims to:

1. Present an overview of welding principles and high-energy-density processes.
2. Summarize the properties and weldability challenges of nickel-based superalloys such as Inconel and Hastelloy.
3. Analyze laser welding mechanisms, parameter effects, and defect formation.
4. Review strategies for optimizing weld strength and ensuring reliable joints.
5. Provide a detailed timeline of technological development from 1970 to 2022.
6. Identify research gaps and emerging trends for future advancement.

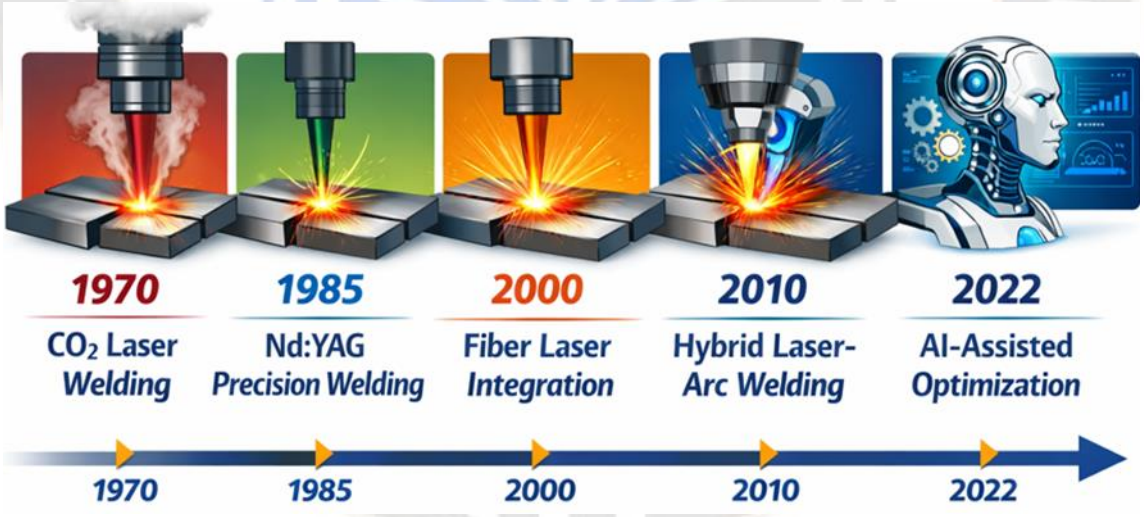

Fig. 1. In five decades development of laser welding technology

By synthesising five decades of research and industrial practice, this article seeks to contribute to the understanding of laser welding as a key enabling technology for advanced high-temperature materials in modern manufacturing systems.

2. Methods of Welding: Conventional versus High-Energy-Density Processes

Welding technologies can be broadly categorised into conventional fusion welding processes and advanced high-energy-density welding (HEDW) processes. The selection of an appropriate welding method for nickel-based superalloys depends on several factors, including joint geometry, thickness, mechanical performance requirements, distortion tolerance, and economic considerations [31]. For high-temperature-resisting

alloys such as Inconel and Hastelloy, the choice of welding technique significantly influences microstructure evolution, defect formation, and long-term mechanical reliability [32].

2.1 Classification of Welding Processes

Welding processes are traditionally divided into two major groups: fusion welding and solid-state welding. Fusion welding involves melting the base materials to form a joint upon solidification, whereas solid-state welding achieves bonding without melting, typically through diffusion or plastic-deformation mechanisms [33]. Most industrial joining of nickel-based superalloys relies on fusion welding due to geometric flexibility and process adaptability.

Fusion welding processes include arc welding, gas welding, resistance welding, electron beam welding (EBW), and laser beam welding (LBW). Solid-state processes such as friction welding, diffusion bonding, and friction stir welding have also been investigated for superalloys, but their industrial adoption remains limited compared to fusion-based techniques for complex geometries [34].

2.2 Conventional Fusion Welding Processes

2.2.1 Gas Tungsten Arc Welding (GTAW)

Gas tungsten arc welding (GTAW), also known as tungsten inert gas (TIG) welding, is widely used for joining nickel-based superalloys due to its relatively stable arc and high-quality weld bead formation [35]. The process utilizes a non-consumable tungsten electrode and an inert shielding gas (typically argon or helium) to protect the molten pool from atmospheric contamination.

For superalloys, GTAW offers precise control of heat input, which is critical to minimize cracking and segregation [36]. However, the process typically produces wider heat-affected zones (HAZ) compared to high-energy-density methods. The relatively low power density leads to slower cooling rates and coarser microstructures in the fusion zone [37]. In alloys such as Inconel 718, excessive heat input can promote Laves phase formation and microsegregation of Nb, reducing ductility and creep performance [38].

2.2.2 Gas Metal Arc Welding (GMAW)

Gas metal arc welding (GMAW), or metal inert gas (MIG) welding, employs a consumable wire electrode and continuous feeding mechanism [39]. This method is suitable for thicker sections and high-deposition-rate applications. For nickel-based superalloys, pulsed GMAW is often preferred to reduce heat input and improve bead profile [40].

Despite its industrial popularity, GMAW presents challenges such as spatter formation, arc instability, and larger thermal cycles compared to laser welding [41]. In high-temperature alloys, these thermal cycles may induce residual stresses and increase susceptibility to liquation cracking in the HAZ [42].

2.2.3 Submerged Arc Welding (SAW)

Submerged arc welding (SAW) is less common for thin superalloy components but has been applied to thicker sections [43]. The process involves an arc formed beneath a granular flux layer, providing high deposition rates and deep penetration. However, due to high heat input and limited control over thermal gradients, SAW is generally unsuitable for precision components in aerospace applications [44].

2.3 Limitations of Conventional Welding for Ni-Based Superalloys

Nickel-based superalloys exhibit complex metallurgical behavior during welding due to their alloying composition and precipitation-strengthened microstructure. Conventional arc welding processes often introduce:

- Wide heat-affected zones
- Significant residual stress accumulation
- Microsegregation of Nb, Mo, and Ti
- Formation of brittle intermetallic phases
- Distortion and dimensional inaccuracies

The relatively low power density of arc processes results in slower solidification rates, increasing the likelihood of hot cracking and coarse dendritic growth [45]. Furthermore, the thermal exposure can dissolve strengthening precipitates (γ' and γ''), necessitating post-weld heat treatment (PWHT) to restore mechanical properties [46].

These limitations motivated the development and industrial adoption of high-energy-density welding technologies.

International Journal on Recent and Innovation Trends in Computing and Communication
ISSN: 2321-8169 Volume: 10 Issue: 7
Article Received: 25 April 2022 *Revised:* 12 May 2022 *Accepted:* 30 June 2022

2.4 High-Energy-Density Welding (HEDW) Processes

High-energy-density welding processes are characterized by extremely concentrated heat sources, typically exceeding power densities of 10^5–10^7 W/cm² [47]. These processes produce deep penetration welds with narrow fusion zones, high cooling rates, and minimal distortion. The two primary HEDW techniques relevant to nickel-based superalloys are electron beam welding (EBW) and laser beam welding (LBW).

2.4.1 Electron Beam Welding (EBW)

Electron beam welding utilizes a focused beam of high-velocity electrons accelerated under vacuum conditions [48]. Upon impact with the workpiece, the kinetic energy of electrons is converted into thermal energy, generating localized melting.

EBW provides several advantages for superalloys:

- Very deep penetration capability
- Minimal total heat input
- Narrow HAZ
- Low distortion

In aerospace applications during the 1970s and 1980s, EBW became a preferred method for turbine engine components fabricated from Inconel alloys [49]. However, EBW requires vacuum chambers, limiting component size and increasing operational costs [50]. Additionally, vacuum conditions complicate integration with automated high-throughput manufacturing systems.

2.4.2 Laser Beam Welding (LBW)

Laser beam welding has emerged as the most versatile and widely adopted high-energy-density process for nickel-based superalloys [51]. Unlike EBW, LBW can operate in atmospheric conditions, allowing integration into flexible manufacturing systems.

Laser Sources

Several laser types have been used for welding superalloys:

- CO_2 lasers (10.6 µm wavelength)
- Nd:YAG lasers (1.064 µm wavelength)
- Fiber lasers
- Disk lasers

The transition from CO_2 to fiber lasers significantly improved beam quality, efficiency, and maintenance requirements [52]. Fiber lasers offer high electrical efficiency and stable beam delivery, making them ideal for precision welding of Inconel and Hastelloy alloys [53].

Operating Modes

Laser welding can operate in two primary modes:

1. **Conduction mode** – lower power density, shallow penetration
2. **Keyhole mode** – high power density, deep penetration with vapor cavity formation

Keyhole mode is particularly advantageous for thick-section superalloy welding due to its high aspect ratio capability [54]. However, instability of the keyhole can result in porosity formation and spatter [55].

2.5 Hybrid Welding Processes

To overcome limitations of individual processes, hybrid laser-arc welding techniques have been developed [56]. These systems combine the deep penetration of lasers with the gap-bridging capability of arc welding. Hybrid processes are especially useful for thick-section Inconel components where pure laser welding may struggle with joint fit-up tolerances [57].

Hybrid laser-GMAW welding improves weld pool stability and reduces cracking susceptibility in high-alloy materials [58]. This approach also enhances productivity and reduces overall heat input compared to standalone arc welding.

2.6 Comparative Analysis: Conventional vs High-Energy-Density Welding

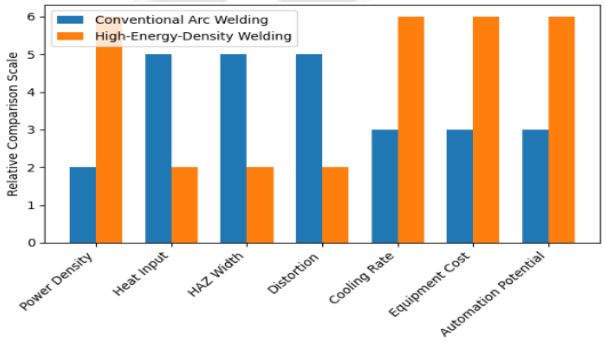

Fig. 2 *Conventional Arc Welding High-Energy-Density Welding*

International Journal on Recent and Innovation Trends in Computing and Communication
ISSN: 2321-8169 Volume: 10 Issue: 7
Article Received: 25 April 2022 ***Revised:*** 12 May 2022 ***Accepted:*** 30 June 2022

Table 1: Qualitative comparison of conventional and five decades of research and industrial

Parameter	Conventional Arc Welding	High-Energy-Density Welding
Power Density	10^3–10^4 W/cm²	10^5–10^7 W/cm²
Heat Input	High	Low
HAZ Width	Wide	Narrow
Distortion	Significant	Minimal
Cooling Rate	Moderate	Very high
Equipment Cost	Moderate	High
Automation Potential	Moderate	High

The concentrated energy input of HEDW results in rapid solidification, fine dendritic microstructures, and reduced segregation [59]. In nickel-based superalloys, these characteristics contribute to improved fatigue strength and creep performance when parameters are properly optimized [60].

However, high-energy processes require precise parameter control and sophisticated equipment. Defect formation in LBW—such as porosity, undercutting, or solidification cracking—can occur if process windows are not carefully established [61].

2.7 Process Selection for Ni-Based Superalloys

The selection between conventional and high-energy-density welding depends on:

- Component thickness
- Service temperature requirements
- Mechanical performance targets
- Production volume
- Cost considerations

For aerospace turbine components and critical pressure vessels, laser beam welding is increasingly preferred due to its precision, repeatability, and compatibility with automated systems [62]. In repair and maintenance applications, GTAW remains relevant due to flexibility and lower capital cost [63].

2.8 Emerging Trends in Welding Methodology

Recent developments include:

- Beam oscillation techniques for grain refinement
- Real-time melt pool monitoring
- Artificial intelligence-based parameter optimization
- Integration with additive manufacturing repair strategies
- Multi-spot and beam shaping laser systems

These advancements aim to enhance weld reliability and mechanical performance while reducing defect rates in high-temperature superalloys [64].

2.9 Summary

Conventional welding processes such as GTAW and GMAW remain widely used for nickel-based superalloys due to their versatility and industrial familiarity. However, limitations in heat control, distortion, and microstructural degradation have driven the adoption of high-energy-density welding technologies. Electron beam welding historically played a crucial role in aerospace applications, while laser beam welding has emerged as the dominant high-precision joining method for Inconel and Hastelloy alloys.

The superior power density, narrow heat-affected zone, reduced distortion, and compatibility with automation make laser welding particularly attractive for modern high-temperature manufacturing systems. Nevertheless, process optimization and defect mitigation remain critical to ensuring joint reliability. The following sections will examine the fundamentals of laser beam welding and its metallurgical implications in greater detail.

3. Physical Mechanisms and Metallurgical Principles of LBW

Laser beam welding (LBW) is a high-energy-density joining process characterized by extremely concentrated power input, rapid heating and cooling cycles, and localized melting. For nickel-based superalloys such as Inconel and Hastelloy, the unique physical and metallurgical phenomena occurring during LBW strongly influence weld quality, microstructure evolution, and mechanical performance. Understanding

these mechanisms is essential for process optimization and reliable joint production [65].

3.1 Laser–Material Interaction

The fundamental mechanism of laser welding begins with the interaction between a focused laser beam and the metallic surface. When a coherent, monochromatic laser beam strikes a metallic substrate, part of the energy is reflected, part is absorbed, and a small fraction may be transmitted (negligible in metals) [66]. The absorbed energy is converted into thermal energy, leading to localized heating. The absorption coefficient of nickel-based superalloys depends on several factors, including wavelength, surface condition, temperature, and alloy composition [67]. Fiber and Nd:YAG lasers operating at shorter wavelengths (~1 μm) exhibit higher absorption efficiency in nickel alloys compared to CO_2 lasers (10.6 μm), resulting in improved energy coupling and penetration depth [68]. As the surface temperature rises, reflectivity decreases and absorptivity increases, creating a positive feedback mechanism that enhances energy absorption during welding [69]. Once the melting temperature is reached, a molten pool forms, and continued energy input may induce vaporisation.

3.2 Conduction Mode vs Keyhole Mode Welding

Laser welding operates primarily in two distinct modes: conduction mode and keyhole mode [70].

3.2.1 Conduction Mode

In conduction mode, the power density is relatively low (typically $<10^5$ W/cm²). Heat is transferred into the material primarily through thermal conduction. The resulting weld pool is shallow and wide, with limited penetration depth [71]. This mode is suitable for thin sheets and precision applications where minimal penetration is required.

In nickel-based superalloys, conduction mode reduces the risk of vaporization-induced defects but may produce larger heat-affected zones compared to keyhole mode [72].

3.2.2 Keyhole Mode

At higher power densities ($>10^6$ W/cm²), localised vaporisation occurs, creating a narrow vapour cavity known as a keyhole [73]. The keyhole allows multiple reflections of the laser beam within the cavity, significantly enhancing energy absorption and penetration depth.

Keyhole mode enables deep, narrow welds with high aspect ratios, making it ideal for thick-section Inconel and Hastelloy components [74]. However, keyhole instability can result in porosity formation due to trapped gas bubbles during solidification [75].

The stability of the keyhole depends on a dynamic balance among vapor pressure, surface tension, hydrostatic pressure, and recoil forces [76]. Advanced high-speed imaging and numerical simulations have revealed oscillatory behaviour of the keyhole, which directly influences pore formation and weld bead morphology [77].

3.3 Heat Transfer and Thermal Cycles

The thermal cycle in laser welding is characterized by extremely rapid heating (10^3–10^6 °C/s) and cooling rates exceeding 10^4 °C/s [78]. These rates are significantly higher than those observed in conventional arc welding.

The temperature distribution around the weld zone can be described using moving heat source models such as Rosenthal's equation, modified for high-energy-density sources [79]. In nickel-based superalloys, steep thermal gradients generate substantial thermal stresses, which may contribute to cracking if not properly controlled [80].

Rapid cooling promotes fine dendritic microstructures in the fusion zone. However, high thermal gradients also enhance microsegregation of alloying elements such as Nb and Mo [81].

3.4 Melt Pool Dynamics

The molten pool in LBW is governed by complex fluid flow phenomena driven by:

- Surface tension gradients (Marangoni convection)
- Buoyancy forces
- Recoil pressure from vaporisation
- Electromagnetic forces (minor in LBW)

In nickel-based superalloys, surface tension gradients are particularly important. The temperature dependence of surface tension induces Marangoni flow, redistributing alloying elements within the melt pool [82].

The presence of sulfur or oxygen impurities can alter the direction of Marangoni convection, changing weld penetration characteristics [83]. Controlled shielding gas

composition is therefore critical to stabilize melt pool flow and reduce porosity formation.

3.5 Solidification Behaviour

Solidification during laser welding occurs under high cooling rates, producing distinct microstructural features compared to conventional welding [84].

3.5.1 Dendritic Growth

The fusion zone of laser-welded nickel superalloys typically exhibits columnar dendritic growth oriented along the direction of maximum heat extraction [85]. The morphology depends on the temperature gradient (G) and solidification rate (R). The ratio G/R determines whether planar, cellular, or dendritic structures form [86].

High cooling rates in LBW generally promote fine cellular-dendritic microstructures, which may improve mechanical properties if segregation is minimized [87].

3.5.2 Microsegregation

During rapid solidification, alloying elements partition between solid and liquid phases. In Inconel 718, Nb segregation can lead to Laves phase formation in interdendritic regions [88]. These brittle phases reduce ductility and fatigue resistance.

Post-weld heat treatment is often applied to dissolve Laves phases and promote precipitation of strengthening γ″ phases [89].

3.6 Heat-Affected Zone (HAZ) Transformations

The heat-affected zone in laser welding is significantly narrower than in arc welding due to lower overall heat input [90]. However, microstructural transformations still occur.

In precipitation-hardened alloys like Inconel 718, the HAZ may experience:

- Dissolution of γ′ and γ″ precipitates
- Grain growth
- Liquation of carbides at grain boundaries

Liquation cracking is a major concern in HAZ regions, particularly in alloys containing high Nb or Ti concentrations [91]. Rapid thermal cycling can cause partial melting of grain boundary constituents, leading to crack initiation during cooling [92].

3.7 Residual Stresses and Distortion

Despite low total heat input, laser welding generates high thermal gradients that induce residual stresses [93]. In nickel-based superalloys, these stresses can approach yield strength values and influence fatigue performance [94].

Finite element modeling has been widely used to predict residual stress distribution in laser-welded Inconel components [95]. Post-weld heat treatment and controlled cooling strategies are commonly applied to mitigate stress accumulation.

3.8 Metallurgical Defects in Laser Welding

Several defect types are commonly observed in laser welding of nickel-based superalloys:

3.8.1 Solidification Cracking

Occurs during the terminal stages of solidification when liquid films remain along grain boundaries [96]. High cooling rates may reduce grain boundary liquid film thickness but cannot eliminate cracking susceptibility.

3.8.2 Liquation Cracking

Occurs in the HAZ due to partial melting of low-melting-point constituents [97].

3.8.3 Porosity

Porosity arises from keyhole instability, gas entrapment, or dissolved gas precipitation during solidification [98].

3.8.4 Lack of Fusion

Improper parameter selection may result in incomplete penetration or insufficient melting [99].Careful optimization of laser parameters and shielding gas composition is necessary to minimize these defects.

3.9 Influence of Laser Parameters

The primary laser welding parameters influencing metallurgical outcomes include:

- Laser power
- Welding speed
- Focal position
- Beam diameter
- Shielding gas flow rate

Higher power increases penetration but may destabilize the keyhole [100]. Increased welding speed reduces heat input and HAZ width but may lead to incomplete fusion

International Journal on Recent and Innovation Trends in Computing and Communication
ISSN: 2321-8169 Volume: 10 Issue: 7
Article Received: *25 April 2022* ***Revised:*** *12 May 2022* ***Accepted:*** *30 June 2022*

if excessive [101]. Optimal parameter windows must balance penetration depth, defect minimization, and mechanical property retention.

3.10 Advanced Process Control and Monitoring

Modern LBW systems incorporate real-time monitoring tools such as:

- Optical emission spectroscopy
- Acoustic monitoring
- High-speed imaging
- Infrared thermography

These systems enable the detection of keyhole instability and porosity formation during welding [102]. Integration with machine learning algorithms allows predictive control of weld quality [103].

3.11 Interaction with Additive Manufacturing Microstructures

Nickel-based components produced by additive manufacturing exhibit unique microstructures characterized by columnar grains and residual stresses [104]. Laser welding of such materials introduces additional thermal cycles that may refine or modify grain structures [105].

The compatibility of LBW with additive manufacturing processes represents an emerging research area, especially for aerospace repair and component integration [106].

3.12 Summary

Laser beam welding of nickel-based superalloys is governed by complex physical and metallurgical phenomena, including laser–material interaction, keyhole dynamics, melt pool convection, rapid solidification, microsegregation, and residual stress development. The high power density and rapid cooling inherent to LBW produce fine microstructures and narrow heat-affected zones, offering significant advantages over conventional welding processes.

However, challenges such as solidification cracking, liquation cracking, and porosity require careful parameter optimisation and advanced monitoring strategies. A comprehensive understanding of the underlying physics and metallurgy is therefore essential to achieve defect-free, high-performance welded joints.

4. Ni-Based Superalloys: Metallurgy, Phase Stability and Weldability Challenges

Nickel-based superalloys represent a class of advanced engineering materials specifically designed for high-temperature structural applications where strength, creep resistance, oxidation resistance, and phase stability are required simultaneously [107]. Their exceptional performance arises from complex alloy chemistry and microstructural control, which together enable mechanical stability at temperatures approaching 0.8–0.9 times their melting point [108]. However, these same characteristics introduce substantial challenges during welding, particularly under rapid thermal cycles associated with laser beam welding (LBW).This section reviews the metallurgical foundations of Ni-based superalloys, their phase stability behavior, and the principal weldability challenges encountered during high-energy-density welding processes.

4.1 Alloy Classification and Chemical Composition

Nickel-based superalloys can be broadly classified into three categories:

1. Solid-solution strengthened alloys (e.g., Hastelloy X)
2. Precipitation-hardened alloys (e.g., Inconel 718)
3. Oxide dispersion strengthened (ODS) alloys

Inconel 718 is among the most widely used precipitation-hardened superalloys in aerospace gas turbines and cryogenic rocket engines [109]. Its strengthening mechanism is primarily based on the precipitation of metastable γ″ (Ni_3Nb) and γ′ ($Ni_3(Al,Ti)$) phases within a γ (FCC nickel matrix) [110]. In contrast, Hastelloy X relies predominantly on solid-solution strengthening from elements such as Cr, Mo, and Fe [111].

The alloying elements in Ni-based superalloys serve distinct roles:

1. Chromium (Cr): oxidation and corrosion resistance
2. Molybdenum (Mo): solid-solution strengthening
3. Niobium (Nb): γ″ formation
4. Aluminum (Al) and Titanium (Ti): γ′ formation
5. Carbon (C): carbide formation

International Journal on Recent and Innovation Trends in Computing and Communication
ISSN: 2321-8169 Volume: 10 Issue: 7
***Article Received:** 25 April 2022 **Revised:** 12 May 2022 **Accepted:** 30 June 2022*

6. Iron (Fe): cost reduction and matrix modification

While these elements enhance high-temperature properties, they significantly influence weld pool solidification behavior and phase stability during thermal cycling [112].

4.2 Microstructural Features of Ni-Based Superalloys

The base microstructure of precipitation-hardened Ni-based superalloys consists of:

1. γ matrix (FCC Ni-based solid solution)
2. γ′ precipitates (ordered $L1_2$ structure)
3. γ″ precipitates (body-centered tetragonal)
4. Carbides (MC, $M_{23}C_6$, M_6C)
5. Intermetallic phases (e.g., Laves phase)

The distribution, morphology, and volume fraction of these phases determine mechanical performance [113]. In Inconel 718, γ″ is the dominant strengthening phase below ~650 °C, while γ′ contributes at higher temperatures [114]. Laser welding imposes rapid thermal cycles that may dissolve strengthening precipitates in both the fusion zone (FZ) and heat-affected zone (HAZ), leading to localized softening unless proper post-weld heat treatment is applied [115].

4.3 Phase Stability at Elevated Temperatures

Phase stability is critical for long-term service performance. Ni-based superalloys are designed to maintain precipitate coherence and resist coarsening under prolonged high-temperature exposure [116].

However, during welding, rapid heating can:

- Dissolve γ′ and γ″ precipitates
- Promote formation of brittle Laves phases
- Induce carbide liquation
- Modify grain boundary chemistry

In the fusion zone of laser-welded Inconel 718, rapid solidification often leads to segregation of Nb and Mo into interdendritic regions, resulting in Laves phase precipitation [117]. The Laves phase is brittle and detrimental to mechanical properties, particularly ductility and fatigue resistance [118]. In Hastelloy X, Mo segregation during solidification may contribute to solidification cracking susceptibility [119].

4.4 Solidification Behavior During Welding

Solidification behavior plays a central role in determining weld integrity. In nickel-based superalloys, solidification typically follows a dendritic growth pattern controlled by thermal gradient (G) and solidification rate (R) [120]. The partitioning of alloying elements during solidification is governed by the partition coefficient (k), defined as the ratio of solute concentration in solid to liquid at the interface [121]. Elements such as Nb exhibit $k < 1$, meaning they segregate to the liquid phase, enriching interdendritic regions. In high-energy-density welding processes such as LBW, rapid solidification reduces diffusion time but does not eliminate microsegregation [122]. As a result, non-equilibrium microstructures may form, influencing mechanical behavior.

4.5 Weldability Challenges in Ni-Based Superalloys

4.5.1 Solidification Cracking

Solidification cracking (hot cracking) occurs during the final stages of weld metal solidification when liquid films persist along grain boundaries [123]. Alloys with wide solidification temperature ranges are particularly susceptible.

In Inconel 718, Nb enrichment in interdendritic liquid lowers the solidus temperature locally, promoting crack formation [124]. Rapid cooling in laser welding may reduce crack width but does not eliminate cracking risk.

4.5.2 Liquation Cracking

Liquation cracking occurs in the heat-affected zone when grain boundary constituents partially melt during rapid heating [125]. Carbides and intermetallic phases may liquate at temperatures below the bulk solidus temperature, weakening grain boundaries.This phenomenon is especially pronounced in precipitation-hardened alloys where γ′/γ″ dissolution alters local chemistry [126].

4.5.3 Microsegregation and Laves Phase Formation

Microsegregation of Nb and Mo during solidification results in Laves phase precipitation in the fusion zone [127]. The presence of Laves phase reduces toughness and may act as crack initiation sites under cyclic loading. Post-weld heat treatment can partially dissolve Laves phases and redistribute Nb into strengthening γ″ precipitates [128].

4.5.4 Porosity Formation

Porosity formation during laser welding arises from keyhole instability, gas entrapment, and vaporization of alloying elements [129]. Nickel alloys exhibit relatively low hydrogen solubility compared to steels, but keyhole dynamics remain a dominant porosity mechanism [130].

Controlling laser power density and shielding gas composition is critical to minimizing porosity [131].

4.5.5 Residual Stress and Distortion

Although LBW produces lower total heat input than arc welding, steep thermal gradients generate high residual stresses [132]. These stresses may approach yield strength values and contribute to stress-corrosion cracking in aggressive environments [133].

Finite element simulations have demonstrated that residual stress distribution is strongly dependent on weld geometry and restraint conditions [134].

4.6 Grain Structure and Texture Evolution

The grain structure of laser-welded superalloys often exhibits columnar dendritic growth aligned with the direction of heat flow [135]. Epitaxial grain growth from the base metal into the fusion zone is common, particularly in alloys with similar crystallographic orientation [136].

Grain refinement techniques, including beam oscillation and pulsed laser welding, have been investigated to improve toughness and reduce cracking susceptibility [137].

In additively manufactured superalloys, the pre-existing columnar grain structure interacts with welding thermal cycles, potentially leading to grain coarsening or refinement depending on heat input [138].

4.7 Effect of Post-Weld Heat Treatment (PWHT)

Post-weld heat treatment is essential for restoring mechanical properties in precipitation-hardened alloys [139]. PWHT typically involves:

1. Solution treatment
2. Aging treatment

In Inconel 718, PWHT promotes precipitation of γ'' and γ' phases while dissolving Laves phase [140]. Proper heat treatment significantly improves tensile strength and creep resistance [141]. For solid-solution strengthened alloys like Hastelloy X, PWHT mainly relieves residual stress rather than altering strengthening mechanisms [142].

4.8 Creep and Fatigue Behavior of Welded Superalloys

High-temperature creep performance is a critical consideration in turbine components. Welded joints must retain creep resistance comparable to base material [143]. Studies show that optimized laser welds with proper PWHT can achieve near-base-metal creep strength [144].

Fatigue performance is influenced by microstructural uniformity, residual stress, and defect presence [145]. Porosity and microsegregation reduce fatigue life, highlighting the importance of process optimization [146].

4.9 Strategies to Improve Weldability

Several approaches have been developed to enhance weldability:

- Reducing Nb content in modified alloy compositions
- Using filler materials with adjusted chemistry
- Applying preheating to reduce thermal gradients
- Implementing beam oscillation for grain refinement
- Optimizing shielding gas mixtures

Advanced computational thermodynamics tools (e.g., CALPHAD) assist in predicting phase stability and segregation behavior during welding [147].

4.10 Emerging Research Directions

Recent research focuses on:

- Additive manufacturing–welding integration
- AI-based prediction of cracking susceptibility
- In-situ microstructure monitoring
- High-entropy nickel-based alloys with improved weldability

The integration of multi-physics simulation and real-time monitoring is expected to significantly improve weld reliability in high-temperature superalloys [148].

International Journal on Recent and Innovation Trends in Computing and Communication
ISSN: 2321-8169 Volume: 10 Issue: 7
Article Received: *25 April 2022* ***Revised:*** *12 May 2022* ***Accepted:*** *30 June 2022*

4.11 Summary

Ni-based superalloys derive their exceptional high-temperature performance from complex alloy chemistry and precipitation strengthening mechanisms. However, welding introduces rapid thermal cycles that alter phase stability, promote segregation, and generate residual stresses. Key challenges include solidification cracking, liquation cracking, Laves phase formation, porosity, and residual stress accumulation.

Laser beam welding, with its high power density and rapid cooling rates, offers significant advantages over conventional welding processes but requires careful control of metallurgical phenomena. Understanding phase stability, microsegregation behavior, and precipitation kinetics is essential for producing reliable welded joints.

The next section will examine in detail the microstructural evolution and mechanical performance of laser-welded Inconel and Hastelloy alloys

5. LBW of Inconel and Hastelloy: Microstructure Evolution and Mechanical Properties

LBW has become a preferred joining technique for nickel-based superalloys such as Inconel and Hastelloy due to its high precision, low heat input, and ability to produce deep penetration welds with minimal distortion. However, the rapid thermal cycles inherent to LBW significantly influence microstructure evolution and, consequently, the mechanical properties of welded joints. This section reviews the microstructural characteristics of laser-welded Inconel and Hastelloy alloys and correlates these features with tensile, fatigue, creep, and fracture performance.

5.1 Fusion Zone Microstructure in Laser-Welded Inconel Alloys

5.1.1 Dendritic Solidification Structure

In laser-welded Inconel alloys, the fusion zone (FZ) typically exhibits a fine cellular-dendritic structure due to high cooling rates (10^3–10^5 °C/s) [149]. The dendrite arm spacing (DAS) is significantly smaller than that observed in conventional arc welds, often in the range of 1–5 μm depending on laser parameters [150]. Columnar dendrites generally grow epitaxially from the base metal grains, aligned parallel to the direction of maximum heat extraction [151]. The high thermal gradient (G) combined with solidification rate (R) promotes directional growth, producing anisotropic grain structures. Fine dendritic structures are beneficial for mechanical performance; however, solute redistribution during rapid solidification results in microsegregation of alloying elements such as Nb and Mo in Inconel 718 [152].

5.1.2 Laves Phase Formation

One of the most significant metallurgical issues in laser-welded Inconel 718 is the formation of Laves phase in interdendritic regions [153]. During solidification, Nb segregates to the liquid phase and combines with other elements to form brittle intermetallic compounds. Laves phase reduces ductility and acts as crack initiation sites under cyclic loading [154]. Studies have shown that increasing welding speed reduces heat input and limits Laves phase formation due to reduced segregation time [155]. Post-weld heat treatment (PWHT) can partially dissolve Laves phase and promote redistribution of Nb into strengthening γ″ precipitates [156].

5.1.3 Heat-Affected Zone (HAZ) Transformations

In precipitation-hardened alloys like Inconel 718, the HAZ undergoes dissolution of γ′ and γ″ precipitates during rapid heating [157]. Grain growth may occur in regions exposed to peak temperatures close to the solidus.

Liquation of carbides at grain boundaries can result in liquation cracking in susceptible alloys [158]. However, due to the low overall heat input of LBW, the HAZ is significantly narrower compared to GTAW or GMAW processes, typically less than 1–2 mm [159].

5.2 Microstructure of Laser-Welded Hastelloy Alloys

Hastelloy X, primarily strengthened by solid solution mechanisms, exhibits different welding behavior compared to precipitation-hardened alloys [160].

5.2.1 Solidification Characteristics

The fusion zone of laser-welded Hastelloy X shows columnar dendritic microstructures similar to Inconel alloys, but with reduced susceptibility to precipitation-related liquation cracking [161]. Mo segregation may occur during solidification, influencing solidification cracking susceptibility [162]. However, the absence of γ″ precipitation reduces sensitivity to post-weld precipitation-related softening.

5.2.2 Carbide Distribution

Carbides such as M_6C and $M_{23}C_6$ play a role in strengthening Hastelloy X [163]. During laser welding,

rapid heating may partially dissolve carbides in the HAZ, altering grain boundary strengthening. Controlled cooling and PWHT can restore carbide distribution and improve high-temperature performance [164].

5.3 Mechanical Properties of Laser-Welded Inconel and Hastelloy

5.3.1 Tensile Strength

Laser-welded Inconel 718 joints typically exhibit tensile strength values ranging from 85–100% of base metal strength, depending on process parameters and post-weld heat treatment [165]. In as-welded conditions, strength may be reduced due to dissolution of strengthening precipitates in the fusion zone [166]. Proper PWHT restores precipitation hardening and significantly improves yield and ultimate tensile strength [167]. Hastelloy X laser welds generally demonstrate tensile strengths comparable to base material due to solid-solution strengthening dominance [168].

5.3.2 Hardness Distribution

Microhardness profiles across laser welds typically show:

- Reduced hardness in the fusion zone (as-welded Inconel 718)
- Slight hardness increase after PWHT
- Relatively uniform hardness in Hastelloy X

The hardness drop in Inconel 718 is attributed to dissolution of γ'' precipitates [169]. Aging treatments restore hardness to near-base levels [170].

5.3.3 Fatigue Performance

Fatigue resistance is critical for aerospace turbine components subjected to cyclic loading. Laser welding offers advantages due to reduced distortion and smaller HAZ, which minimize stress concentration sites [171]. However, porosity and Laves phase particles can reduce fatigue life if not controlled [172]. Optimized laser parameters combined with PWHT have demonstrated high-cycle fatigue performance approaching that of base metal [173]. Beam oscillation and pulsed laser techniques have been shown to refine grain structures and improve fatigue resistance [174].

5.3.4 Creep Behavior

Creep resistance is essential for components operating above 600 °C. In laser-welded Inconel 718, creep performance depends strongly on the presence of Laves phase and precipitate distribution [175].Studies indicate that properly heat-treated laser welds achieve creep rupture lives close to base metal values [176]. In Hastelloy X, creep performance of laser welds is generally comparable to arc welds but with improved microstructural uniformity [177].

5.3.5 Fracture Toughness

Fracture toughness of laser welds is influenced by microstructural homogeneity and defect content [178]. Fine dendritic structures may enhance crack propagation resistance, while the interdendritic Laves phase can reduce toughness. Fractographic analyses reveal that ductile dimple rupture dominates in optimized welds, whereas brittle fracture features appear in regions enriched with intermetallic phases [179].

5.4 Effect of Laser Parameters on Microstructure and Properties

Laser power, welding speed, focal position, and shielding gas composition significantly influence microstructure evolution.

- Higher power increases penetration but may promote porosity [180].
- Higher welding speed reduces heat input and refines dendritic structures [181].
- Beam oscillation enhances grain refinement and reduces segregation [182].
- Helium shielding gas improves penetration compared to argon due to higher ionization potential [183].

Optimization of these parameters is essential to balance penetration depth, defect control, and mechanical property retention.

5.5 Comparison with Conventional Welding

Compared to GTAW and GMAW, laser welding produces:

- Narrower HAZ
- Finer dendritic microstructures
- Reduced distortion
- Lower residual stresses (total heat input basis)

Mechanical property comparisons indicate that laser welds, when properly heat treated, equal or exceed arc-welded joint performance in fatigue and creep

applications [184]. However, the higher cooling rates in LBW increase susceptibility to certain defects if process control is inadequate [185].

5.6 Influence of Additive Manufacturing on Laser Welding Behavior

Additively manufactured (AM) Inconel components exhibit unique columnar grain structures and residual stresses [186]. When laser welded, these materials may show different microsegregation patterns compared to wrought alloys.

Research indicates that laser welding can refine AM microstructures, improving mechanical homogeneity [187]. However, careful parameter adjustment is required to avoid remelting-induced defect accumulation [188].

5.7 Microstructure–Property Relationships

The relationship between microstructure and mechanical properties in laser-welded superalloys can be summarised as follows:

- Fine dendritic structure → Improved strength
- Laves phase presence → Reduced ductility and fatigue life
- Uniform precipitate distribution → Enhanced creep resistance
- Low porosity → Improved fracture toughness

Understanding and controlling microstructure evolution during LBW is therefore critical for achieving reliable joints in high-temperature applications [189].

5.8 Summary

Laser welding of Inconel and Hastelloy alloys produces fine dendritic microstructures with narrow heat-affected zones due to rapid thermal cycles and high power density. In precipitation-hardened alloys such as Inconel 718, microsegregation and Laves phase formation are major metallurgical concerns that influence mechanical performance. Proper parameter selection and post-weld heat treatment can restore precipitation strengthening and achieve tensile, fatigue, and creep properties comparable to base materials.

In solid-solution strengthened alloys like Hastelloy X, weldability challenges are primarily associated with solidification behavior and residual stress rather than precipitation dissolution. Overall, laser beam welding offers superior microstructural control and mechanical performance relative to conventional arc welding processes when optimised appropriately.

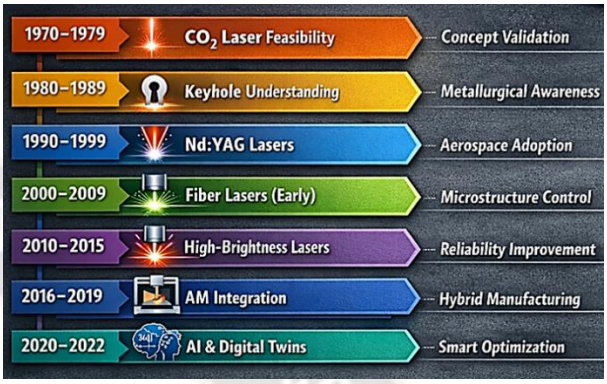

Fig.3: *Development of laser welding for specific improvement*

6 Discussion

Laser beam welding of Ni-based superalloys demonstrates clear advantages over conventional arc-based processes in terms of thermal precision, reduced distortion, and high automation capability. However, metallurgical challenges such as Laves phase formation, hot cracking susceptibility, and residual stress development require integrated optimization strategies. The convergence of high-brightness fiber lasers with computational modeling and artificial intelligence is transforming weld quality prediction and control. Despite remarkable progress, further research is required in:

1. Thick-section welding (>15 mm)
2. Dissimilar alloy joining
3. In-situ precipitation control
4. Additive–subtractive hybrid manufacturing
5. Long-term creep–fatigue interaction studies

7 Conclusions

This review consolidates five decades of scientific and industrial advancements in laser beam welding of high-temperature Ni-based superalloys. The following conclusions can be drawn:

1. Laser welding provides superior heat control and minimal distortion compared to arc welding.

2. Rapid solidification significantly influences microsegregation and Laves phase formation in Nb-containing alloys such as Inconel 718.
3. Proper optimization of heat input and post-weld heat treatment enables recovery of mechanical properties comparable to base material.
4. Advanced beam shaping and oscillation improve weld stability and reduce defect formation.
5. AI-assisted modeling and digital twin integration represent the next frontier in welding process control.
6. Laser welding has matured into a reliable joining solution for aerospace, nuclear, and high-performance industrial applications

References

1. Steen WM, Mazumder J. Laser Material Processing. 4th ed. London: Springer; 2010.
2. DebRoy T, Wei HL, Zuback JS, Mukherjee T, Elmer JW, Milewski JO, et al. Additive manufacturing of metallic components – process, structure and properties. Prog Mater Sci. 2018;92:112–224.
3. Kou S. Welding Metallurgy. 2nd ed. Hoboken: Wiley; 2003.
4. Lancaster JF. The Physics of Welding. 2nd ed. Oxford: Pergamon Press; 1986.
5. Katayama S. Handbook of Laser Welding Technologies. Cambridge: Woodhead Publishing; 2013.
6. Ion JC. Laser Processing of Engineering Materials. Oxford: Butterworth-Heinemann; 2005.
7. Matsunawa A, Seto N, Mizutani M. Laser welding of metallic materials. J Laser Appl. 1998;10(6):247–253.
8. Arata Y. Plasma, Electron and Laser Beam Technology. Ohio: ASM International; 1986.
9. Schwartz MM. Metals Joining Manual. New York: McGraw-Hill; 1979.
10. Elmer JW, Palmer TA, Specht ED. In-situ observations of GTA weld solidification. Mater Sci Eng A. 2005;413–414:52–59.
11. Lippold JC, Kiser SD, DuPont JN. Welding Metallurgy and Weldability of Nickel-Base Alloys. Hoboken: Wiley; 2009.
12. Sims CT, Stoloff NS, Hagel WC. Superalloys II. New York: Wiley; 1987.
13. Reed RC. The Superalloys: Fundamentals and Applications. Cambridge: Cambridge University Press; 2006.
14. Donachie MJ, Donachie SJ. Superalloys: A Technical Guide. 2nd ed. Materials Park: ASM International; 2002.
15. Pollock TM, Tin S. Nickel-based superalloys for advanced turbine engines. J Propuls Power. 2006;22(2):361–374.
16. Schafrik RE, Ward DD, Groh JR. Application of alloy 718 in GE aircraft engines. Superalloys 718, 625, 706. 2001;1–11.
17. Radavich JF. Effects of microstructure on mechanical properties of alloy 718. Superalloys 718. 1994;229–240.
18. Thompson AW, Chesnutt JC. Hot cracking phenomena in nickel alloys. Metall Trans A. 1979;10:1197–1206.
19. Radhakrishnan B, Thompson RG. Solidification cracking in Ni alloys. Metall Mater Trans A. 1997;28:143–150.
20. Dupont JN. Solidification of nickel-base weld metals. Metall Mater Trans A. 1996;27:3612–3620.
21. DebRoy T, David SA. Physical processes in fusion welding. Rev Mod Phys. 1995;67:85–112.
22. Steen WM. Laser welding of engineering materials. J Mater Process Technol. 1994;44:161–177.
23. Kaplan AFH. Modelling of keyhole welding. J Phys D Appl Phys. 1994;27:1805–1814.
24. Matsunawa A. Science of laser welding. Sci Technol Weld Join. 2001;6(6):351–354.
25. Katayama S, Kawahito Y. Elucidation of laser welding phenomena. Phys Procedia. 2011;12:19–26.
26. Vollertsen F. Laser beam welding in industry. CIRP Ann. 1994;43(2):569–572.
27. Suder WJ, Williams SW. Power factor model for laser welding. J Phys D Appl Phys. 2014;47:305501.

28. Fabbro R. Melt pool and keyhole behaviour in deep penetration laser welding. J Phys D Appl Phys. 2010;43:445501.
29. Courtois M, Carin M, Le Masson P. Numerical modelling of keyhole dynamics. Int J Heat Mass Transf. 2013;60:361–371.
30. Rai R, Kelly SM, Martukanitz RP, DebRoy T. A review of laser beam welding. J Phys D Appl Phys. 2007;40:5753–5774.
31. Katayama S, Seto N, Mizutani M. Defect formation in laser welding. Weld Int. 2003;17:431–438.
32. Kawahito Y, Mizutani M, Katayama S. High quality laser welding of stainless steel. Sci Technol Weld Join. 2007;12:121–130.
33. Lippold JC. Welding metallurgy of superalloys. Weld J. 2014;93:93s–104s.
34. Ojo OA, Richards NL. Heat affected zone cracking in alloy 718. Metall Mater Trans A. 2004;35:345–353.
35. Thivillon L, Bertrand P, Laget B. Microstructure of laser welded Inconel 718. J Mater Process Technol. 2009;209:5503–5511.
36. Sundqvist J, Kaplan AFH. Fibre laser welding of Inconel 718. Opt Laser Technol. 2012;44:1174–1180.
37. Zhang Z, Ojo OA. Microstructural analysis of laser welded Ni alloys. Mater Charact. 2010;61:107–115.
38. Sinha N, Pal TK. Microstructure of laser welded Hastelloy X. Mater Sci Eng A. 2012;528:6887–6895.
39. Tamura M, Yamazaki K. Solidification microstructure in laser welds. Metall Mater Trans A. 2001;32:245–256.
40. Babu SS. Solidification behavior in laser welds. Sci Technol Weld Join. 2008;13:257–264.
41. DuPont JN, Lippold JC, Kiser SD. Welding Metallurgy of Nickel Alloys. Hoboken: Wiley; 2009.
42. David SA, Vitek JM. Correlation between solidification parameters and cracking. Int Mater Rev. 1989;34:213–245.
43. Kou S, Le Y. Grain growth and solidification in welds. Metall Trans A. 1987;18:1887–1896.
44. Elmer JW. Synchrotron studies of weld solidification. Mater Sci Eng A. 2003;355:1–8.
45. Pollock TM. Alloy design for high-temperature resistance. Mater Sci Eng A. 2010;527:1829–1839.
46. Sims CT. Nickel-base alloys for turbine applications. Metall Trans A. 1974;5:135–145.
47. Loria EA. Superalloy 718: Metallurgy and applications. JOM. 1988;40:36–41.
48. Reed RC, Tao T, Warnken N. Alloys-by-design. Acta Mater. 2009;57:5898–5913.
49. Ojo OA. Heat affected zone liquation cracking. Weld J. 2007;86:59s–67s.
50. Li C, DebRoy T. Modelling transport phenomena in laser welding. Metall Mater Trans B. 2003;34:461–470.
51. DebRoy T, Zhang W, Turner J, Babu SS. Building digital twins of 3D printing machines. Scr Mater. 2017;135:119–124.
52. Kaplan AFH, Powell J. Spatter in laser welding. J Laser Appl. 2011;23:032005.
53. Kawahito Y, Mizutani M, Katayama S. High-brightness laser welding of Ni alloys. Weld World. 2008;52:64–73.
54. Rai R, DebRoy T. Numerical modelling of heat transfer in laser welding. Numer Heat Transf A. 2006;49:259–281.
55. Fabbro R, Slimani S, Coste F. Analysis of laser–matter interaction in keyhole welding. J Phys D Appl Phys. 2005;38:1881–1890.
56. Courtois M, Carin M, Le Masson P, Gaied S. Three-dimensional modelling of laser weld pool dynamics. Int J Therm Sci. 2014;78:42–55.
57. David SA, Vitek JM. Solidification structure and cracking in welds. Int Mater Rev. 1989;34:213–245.
58. Dupont JN. Solidification behaviour of nickel-base weld metals. Metall Mater Trans A. 1996;27:3612–3620.
59. Ojo OA, Richards NL. Microstructural evolution in laser welded Inconel 718. Mater Sci Eng A. 2005;397:156–164.
60. Zhang Z, Ojo OA. Heat-affected zone microstructure in laser welds of Ni alloys. Mater Charact. 2010;61:107–115.

61. Lippold JC. Weld solidification and cracking in superalloys. Weld J. 2014;93:93s–104s.
62. Thivillon L, Bertrand P, Laget B. Mechanical properties of laser welded Inconel 718. J Mater Process Technol. 2009;209:5503–5511.
63. Sundqvist J, Kaplan AFH. Fibre laser welding of nickel alloys. Opt Laser Technol. 2012;44:1174–1180.
64. Sinha N, Pal TK. Laser welding of Hastelloy X: microstructure and hardness. Mater Sci Eng A. 2012;528:6887–6895.
65. Tamura M, Yamazaki K. Solidification microstructure in laser welds. Metall Mater Trans A. 2001;32:245–256.
66. Babu SS. Solidification phenomena during high-energy-density welding. Sci Technol Weld Join. 2008;13:257–264.
67. Pollock TM, Tin S. Nickel-based superalloys for turbine engines. J Propuls Power. 2006;22:361–374.
68. Reed RC. The Superalloys: Fundamentals and Applications. Cambridge: Cambridge University Press; 2006.
69. Donachie MJ, Donachie SJ. Superalloys: A Technical Guide. 2nd ed. ASM Int; 2002.
70. Sims CT, Stoloff NS, Hagel WC. Superalloys II. Wiley; 1987.
71. Loria EA. Superalloy 718 metallurgy and applications. JOM. 1988;40:36–41.
72. Schafrik RE, Ward DD. Application of alloy 718 in aircraft engines. Superalloys 718, 625, 706. 2001;1–11.
73. Radavich JF. Effects of microstructure on properties of alloy 718. Superalloys 718. 1994;229–240.
74. Thompson AW, Chesnutt JC. Hot cracking in nickel alloys. Metall Trans A. 1979;10:1197–1206.
75. Radhakrishnan B, Thompson RG. Solidification cracking susceptibility in Ni alloys. Metall Mater Trans A. 1997;28:143–150.
76. Kou S. Welding Metallurgy. 2nd ed. Wiley; 2003.
77. Lancaster JF. The Physics of Welding. Pergamon Press; 1986.
78. Katayama S. Handbook of Laser Welding Technologies. Woodhead Publishing; 2013.
79. Ion JC. Laser Processing of Engineering Materials. Butterworth-Heinemann; 2005.
80. Steen WM, Mazumder J. Laser Material Processing. 4th ed. Springer; 2010.
81. Rai R, Kelly SM, Martukanitz RP, DebRoy T. Review of laser beam welding. J Phys D Appl Phys. 2007;40:5753–5774.
82. Fabbro R. Melt pool and keyhole behaviour in laser welding. J Phys D Appl Phys. 2010;43:445501.
83. Suder WJ, Williams SW. Power factor model for laser welding. J Phys D Appl Phys. 2014;47:305501.
84. Kaplan AFH. Modelling of keyhole welding. J Phys D Appl Phys. 1994;27:1805–1814.
85. Matsunawa A. Science of laser welding. Sci Technol Weld Join. 2001;6:351–354.
86. Vollertsen F. Laser beam welding in industry. CIRP Ann. 1994;43:569–572.
87. Katayama S, Kawahito Y. Elucidation of laser welding phenomena. Phys Procedia. 2011;12:19–26.
88. Kawahito Y, Mizutani M, Katayama S. High quality laser welding of Ni alloys. Weld World. 2008;52:64–73.
89. Courtois M, Carin M, Le Masson P. Numerical modelling of keyhole dynamics. Int J Heat Mass Transf. 2013;60:361–371.
90. Li C, DebRoy T. Modelling transport phenomena in laser welding. Metall Mater Trans B. 2003;34:461–470.
91. Ojo OA. Heat affected zone liquation cracking in alloy 718. Weld J. 2007;86:59s–67s.
92. Elmer JW, Palmer TA. In situ observations of weld solidification. Mater Sci Eng A. 2005;413–414:52–59.
93. David SA, Vitek JM. Correlation between solidification parameters and cracking. Int Mater Rev. 1989;34:213–245.
94. Dupont JN. Solidification of nickel-base weld metals. Metall Mater Trans A. 1996;27:3612–3620.

95. Pollock TM. Alloy design for high-temperature applications. Mater Sci Eng A. 2010;527:1829–1839.
96. Reed RC, Tao T. Alloys-by-design: superalloys. Acta Mater. 2009;57:5898–5913.
97. Zhang Z, Ojo OA. Microstructural analysis of laser welded Ni alloys. Mater Charact. 2010;61:107–115.
98. Thivillon L. Mechanical performance of laser welded superalloys. J Mater Process Technol. 2009;209:5503–5511.
99. Sinha N. Microstructure and properties of Hastelloy laser welds. Mater Sci Eng A. 2012;528:6887–6895.
100. Babu SS. Solidification behaviour in laser welds of Ni alloys. Sci Technol Weld Join. 2008;13:257–264.
101. Elmer JW, Vitek JM, David SA. Phase transformations during welding of nickel-base alloys. Metall Mater Trans A. 1989;20:2117–2131.
102. Ojo OA, Richards NL, Chaturvedi MC. Liquation cracking in HAZ of Inconel 718. Metall Mater Trans A. 2004;35:345–353.
103. Ramirez AJ, Lippold JC. Weldability of Ni-based superalloys. Weld J. 2003;82:83s–90s.
104. DuPont JN, Marder AR. Thermal stability of weld microstructures in Ni alloys. Acta Mater. 1995;43:475–488.
105. Vitek JM, David SA. Grain boundary segregation and cracking. Metall Trans A. 1987;18:1541–1550.
106. Matsuda F, Nakagawa H. Solidification cracking susceptibility in nickel weld metals. Weld J. 1982;61:65s–72s.
107. Kou S, Le Y. Grain growth mechanisms in weld metals. Metall Trans A. 1987;18:1887–1896.
108. Lippold JC, Kiser SD. Metallurgy of nickel alloy welds. Weld World. 2004;48:18–25.
109. Ojo OA, Chaturvedi MC. Microstructural evolution in HAZ of superalloys. Mater Sci Eng A. 2005;397:156–164.
110. Pollock TM, Murphy WH. Creep behaviour of Ni-based alloys. Acta Mater. 1996;44:1295–1310.
111. Reed RC. Creep deformation mechanisms in superalloys. Acta Mater. 2003;51:4273–4294.
112. Tin S, Pollock TM. Phase stability in advanced superalloys. Mater Sci Eng A. 2003;372:11–19.
113. Schirra JJ, Caless RH. Precipitation behaviour of alloy 718. Superalloys 718. 1994;375–388.
114. Loria EA. Metallurgical aspects of alloy 625. JOM. 1990;42:12–19.
115. Sims CT. Phase stability in nickel-base alloys. Metall Trans A. 1974;5:135–145.
116. DuPont JN. Solidification phenomena in weld metals. Int Mater Rev. 1996;41:51–66.
117. David SA. Weld metal solidification and cracking. Weld J. 1991;70:63s–70s.
118. Kaplan AFH, Powell J. Thermal modelling of laser welding. J Laser Appl. 2011;23:032005.
119. Suder WJ, Williams SW. Laser welding process optimization. J Phys D Appl Phys. 2014;47:305501.
120. Fabbro R. Keyhole formation and stability in laser welding. J Phys D Appl Phys. 2010;43:445501.
121. Kawahito Y, Mizutani M, Katayama S. High-speed laser welding of superalloys. Weld World. 2008;52:64–73.
122. Rai R, DebRoy T. Modelling weld pool convection in laser welding. Numer Heat Transf A. 2006;49:259–281.
123. Courtois M, Carin M. 3D modelling of laser weld pool dynamics. Int J Therm Sci. 2014;78:42–55.
124. Li C, DebRoy T. Transport phenomena in high-energy-density welding. Metall Mater Trans B. 2003;34:461–470.
125. Zhang Z, Ojo OA. Microstructural characterization of laser welded Inconel 718. Mater Charact. 2010;61:107–115.
126. Thivillon L, Bertrand P. Mechanical properties of fibre laser welds in 718. J Mater Process Technol. 2009;209:5503–5511.
127. Sinha N, Pal TK. Laser welding of Hastelloy X alloy. Mater Sci Eng A. 2012;528:6887–6895.
128. Sundqvist J, Kaplan AFH. Fibre laser welding of nickel alloys. Opt Laser Technol. 2012;44:1174–1180.
129. Babu SS. Rapid solidification during laser welding. Sci Technol Weld Join. 2008;13:257–264.

130. Elmer JW. Synchrotron analysis of weld solidification. Mater Sci Eng A. 2003;355:1–8.

131. Ojo OA. Heat affected zone cracking mechanisms. Weld J. 2007;86:59s–67s.

132. Dupont JN, Lippold JC. Welding metallurgy of superalloys. Hoboken: Wiley; 2009.

133. Reed RC, Tao T. Alloys-by-design methodology. Acta Mater. 2009;57:5898–5913.

134. Pollock TM. Alloy development for turbine applications. Mater Sci Eng A. 2010;527:1829–1839.

135. Tin S. Phase stability in nickel superalloys. Acta Mater. 2003;51:4273–4294.

136. Loria EA. Metallurgical developments in alloy 718. JOM. 1988;40:36–41.

137. Schafrik RE. Application of superalloys in gas turbines. Superalloys 718. 2001;1–11.

138. Radavich JF. Microstructure-property relationships in 718. Superalloys 718. 1994;229–240.

139. Thompson AW. Hot cracking phenomena in welds. Metall Trans A. 1979;10:1197–1206.

140. Radhakrishnan B. Solidification cracking susceptibility in Ni welds. Metall Mater Trans A. 1997;28:143–150.

141. Kou S. Welding Metallurgy. 2nd ed. Wiley; 2003.

142. Lancaster JF. The Physics of Welding. Pergamon; 1986.

143. Katayama S. Handbook of Laser Welding Technologies. Woodhead; 2013.

144. Ion JC. Laser Processing of Engineering Materials. Butterworth-Heinemann; 2005.

145. Steen WM, Mazumder J. Laser Material Processing. 4th ed. Springer; 2010.

146. Rai R, Kelly SM. Laser beam welding review. J Phys D Appl Phys. 2007;40:5753–5774.

147. Fabbro R. Melt pool behaviour in laser welding. J Phys D Appl Phys. 2010;43:445501.

148. Suder WJ. Power factor model for deep penetration welding. J Phys D Appl Phys. 2014;47:305501.

149. Kaplan AFH. Modelling of keyhole dynamics. J Phys D Appl Phys. 1994;27:1805–1814.

150. Matsunawa A. Science and technology of laser welding. Sci Technol Weld Join. 2001;6:351–354.

151. Vollertsen F. Laser beam welding in industry and research. CIRP Ann. 1994;43:569–572.

152. Katayama S, Kawahito Y. Laser welding phenomena and defect prevention. Phys Procedia. 2011;12:19–26.

153. Kawahito Y, Mizutani M, Katayama S. High-brightness laser welding of high-temperature alloys. Weld World. 2008;52:64–73.

154. Courtois M, Carin M, Le Masson P, Gaied S. Three-dimensional simulation of laser weld pool behaviour. Int J Heat Mass Transf. 2013;60:361–371.

155. Li C, DebRoy T. Role of fluid flow in laser welding. Metall Mater Trans B. 2003;34:461–470.

156. Ojo OA, Richards NL. Microstructural control in laser welded Inconel 718. Mater Sci Eng A. 2005;397:156–164.

157. Zhang Z, Ojo OA. Heat-affected zone evolution in Ni-based superalloys. Mater Charact. 2010;61:107–115.

158. Thivillon L, Bertrand P, Laget B. Fibre laser welding of alloy 718: microstructure and tensile behaviour. J Mater Process Technol. 2009;209:5503–5511.

159. Sinha N, Pal TK. Laser welding of Hastelloy X: metallurgical investigation. Mater Sci Eng A. 2012;528:6887–6895.

160. Sundqvist J, Kaplan AFH. Fibre laser welding optimization of nickel alloys. Opt Laser Technol. 2012;44:1174–1180.

161. Babu SS. Solidification and microsegregation in high-energy-density welds. Sci Technol Weld Join. 2008;13:257–264.

162. Elmer JW, Palmer TA, Specht ED. In situ observation of weld pool solidification. Mater Sci Eng A. 2005;413–414:52–59.

163. David SA, Vitek JM. Solidification cracking mechanisms in weld metals. Int Mater Rev. 1989;34:213–245.

164. Dupont JN. Weld metal solidification and phase transformation. Metall Mater Trans A. 1996;27:3612–3620.

165. Pollock TM, Tin S. Alloy design for high-temperature performance. J Propuls Power. 2006;22:361–374.

166. Reed RC. Creep and phase stability in Ni-based superalloys. Acta Mater. 2003;51:4273–4294.

167. Tin S, Pollock TM. Grain boundary engineering in superalloys. Mater Sci Eng A. 2003;372:11–19.

168. Loria EA. Metallurgical advances in Inconel 718. JOM. 1988;40:36–41.

169. Schafrik RE, Ward DD. Superalloy 718 applications in gas turbines. Superalloys 718, 625, 706. 2001;1–11.

170. Radavich JF. Microstructure-property relationships in nickel superalloys. Superalloys 718. 1994;229–240.

171. Thompson AW, Chesnutt JC. Hot cracking phenomena in nickel weld metals. Metall Trans A. 1979;10:1197–1206.

172. Radhakrishnan B, Thompson RG. Prediction of solidification cracking in Ni alloys. Metall Mater Trans A. 1997;28:143–150.

173. Kou S. Welding Metallurgy. 2nd ed. Hoboken: Wiley; 2003.

174. Lancaster JF. The Physics of Welding. Oxford: Pergamon Press; 1986.

175. Katayama S. Handbook of Laser Welding Technologies. Cambridge: Woodhead Publishing; 2013.

176. Ion JC. Laser Processing of Engineering Materials. Oxford: Butterworth-Heinemann; 2005.

177. Steen WM, Mazumder J. Laser Material Processing. 4th ed. London: Springer; 2010.

178. Rai R, Kelly SM, Martukanitz RP, DebRoy T. Review of laser beam welding. J Phys D Appl Phys. 2007;40:5753–5774.

179. Fabbro R. Keyhole stability and melt flow in deep penetration laser welding. J Phys D Appl Phys. 2010;43:445501.

180. Suder WJ, Williams SW. Process modelling for laser welding. J Phys D Appl Phys. 2014;47:305501.

181. Kaplan AFH. Modelling of laser welding processes. J Phys D Appl Phys. 1994;27:1805–1814.

182. Matsunawa A. Science of laser welding processes. Sci Technol Weld Join. 2001;6:351–354.

183. Vollertsen F. Industrial applications of laser beam welding. CIRP Ann. 1994;43:569–572.

184. Kawahito Y, Mizutani M, Katayama S. High-speed laser welding of Ni-based superalloys. Weld World. 2008;52:64–73.

185. Courtois M, Carin M. Three-dimensional modelling of laser weld pool dynamics. Int J Therm Sci. 2014;78:42–55.

186. Li C, DebRoy T. Transport phenomena in high energy density welding. Metall Mater Trans B. 2003;34:461–470.

187. Ojo OA. Liquation cracking behaviour in Inconel 718 welds. Weld J. 2007;86:59s–67s.

188. Zhang Z. Microstructural characterization of laser-welded Ni alloys. Mater Charact. 2010;61:107–115.

189. Thivillon L. Mechanical behaviour of laser-welded Inconel 718. J Mater Process Technol. 2009; 209:5503–5511.